RESEARCH PAPER

Nucleus 5:6, 613–625; November/December 2014; © 2014 Taylor & Francis Group, LLC

Drosophila Symplekin localizes dynamically to the histone locus body and tricellular junctions

Deirdre C Tatomer[1], Lindsay F Rizzardi[2], Kaitlin P Curry[2], Alison M Witkowski[1], William F Marzluff[1,2,3,4,5,*], and Robert J Duronio[1,2,3,5,6,*]

[1]Department of Biology; University of North Carolina; Chapel Hill, NC USA; [2]Curriculum in Genetics and Molecular Biology; University of North Carolina; Chapel Hill, NC USA; [3]Integrative Program for Biological & Genome Sciences; University of North Carolina; Chapel Hill, NC USA; [4]Department of Biochemistry and Biophysics; University of North Carolina; Chapel Hill, NC USA; [5]Lineberger Comprehensive Cancer Center; University of North Carolina; Chapel Hill, NC USA; [6]Department of Genetics; University of North Carolina; Chapel Hill, NC USA

Keywords: *Drosophila*, gene expression, histone mRNA, nuclear bodies, RNA processing, Symplekin

Abbreviations: cas, castor; CTD, RNA polymerase II C-terminal domain; HCC, histone cleavage complex; HDE, histone downstream element; HLB, histone locus body; Madm, MLF1-adaptor molecule; PAP, poly (A) polymerase; PAS, poly A signal; Rp49, ribosomal protein L32; SL, stem loop; SLBP, stem loop binding protein; sop, ribosomal protein S2; Sym, Symplekin; yps, ypsilon schachtel.

The scaffolding protein Symplekin is part of multiple complexes involved in generating and modifying the 3′ end of mRNAs, including cleavage-polyadenylation, histone pre-mRNA processing and cytoplasmic polyadenylation. To study these functions *in vivo*, we examined the localization of Symplekin during development and generated mutations of the *Drosophila* Symplekin gene. Mutations in *Symplekin* that reduce Symplekin protein levels alter the efficiency of both poly A^+ and histone mRNA 3′ end formation resulting in lethality or sterility. Histone mRNA synthesis takes place at the histone locus body (HLB) and requires a complex composed of Symplekin and several polyadenylation factors that associates with the U7 snRNP. Symplekin is present in the HLB in the early embryo when Cyclin E/Cdk2 is active and histone genes are expressed and is absent from the HLB in cells that have exited the cell cycle. During oogenesis, Symplekin is preferentially localized to HLBs during S-phase in endoreduplicating follicle cells when histone mRNA is synthesized. After the completion of endoreplication, Symplekin accumulates in the cytoplasm, in addition to the nucleoplasm, and localizes to tricellular junctions of the follicle cell epithelium. This localization depends on the RNA binding protein ypsilon schachtel. CPSF-73 and a number of mRNAs are localized at this same site, suggesting that Symplekin participates in cytoplasmic polyadenylation at tricellular junctions.

Introduction

The development of complex organisms containing a diverse array of multifunctional tissues requires dynamic modulation of gene expression. While transcription regulation is a critical component of gene expression, many additional mechanisms that help control gene expression during development involve the 3′ end of an mRNA, including translational regulation, mRNA localization, production of different isoforms of the same mRNA by alternative splicing or polyadenylation, and regulation of 3′ end formation as a component of histone mRNA synthesis.[1,2]

The 3′ end of most eukaryotic mRNAs is generated by endonucleolytic cleavage followed by addition of a poly(A) tail. The sole known exception is the metazoan replication dependent histone mRNAs, which are not polyadenylated and instead end in a conserved stem loop structure.[2] Cleavage of both types of mRNA is directed by two *cis* elements near the 3′ end of the pre-mRNA. For polyadenylated mRNA, the signals are the AAUAAA poly(A) signal and G/U rich downstream element, with cleavage occurring between the two elements.[3] These *cis* elements assemble the cleavage and polyadenylation machinery, which minimally consists of the scaffolding protein Symplekin and four protein complexes: CPSF, which binds the poly(A) signal, CstF, which binds the G/U rich element, and CF I_m and CF II_m, as well as poly(A) polymerase (PAP).[4] CPSF-73 is the endonuclease that cleaves pre-mRNAs followed by polyadenylation by PAP.[5]

Cleavage of histone pre-mRNA is similarly mediated by two *cis* elements, the stem loop, which binds stem loop binding protein (SLBP), and the histone downstream element (HDE), which binds U7 snRNP.[6-9] The Sm ring of U7 snRNP contains two proteins only found in the U7 sRNP, Lsm10 and Lsm11.[10,11] The N-terminus of Lsm11 binds to FLASH, and this interaction is critical for histone pre-mRNA 3′ end formation.[12,13] The discovery of CPSF-73 as the endonuclease that cleaves histone pre-mRNA provided the first indication that polyadenylation factors were also involved in histone mRNA biosynthesis.[14] Recently,

*Correspondence to: William F Marzluff; Email: marzluff@med.unc.edu; Robert J Duronio; Email: duronio@med.unc.edu
Submitted: 06/25/2014; Revised: 10/17/2014; Accepted: 10/22/2014
http://dx.doi.org/10.4161/19491034.2014.990860

Dominski and coworkers showed that the FLASH and Lsm11 complex binds directly to a subset of polyadenylation factors termed the histone cleavage complex (HCC). The HCC includes Symplekin, CstF64 and the entire CPSF complex. In both mammals and *Drosophila,* the HCC can be isolated as a component of the U7 snRNP, suggesting that the active form of the U7 snRNP complex consists of the core U7snRNP particle plus FLASH and the HCC.[15,16]

Biochemical experiments additionally demonstrated that Symplekin participates in histone pre-mRNA processing. Early characterization of histone pre-mRNA processing indicated that a component of the cleavage machinery was heat sensitive.[17] Almost 20 years later, Kolev and Steitz showed that complementation of a heat-inactivated extract by *in vitro* transcribed and translated Symplekin restored *in vitro* cleavage of a histone pre-mRNA substrate.[18] Furthermore, Symplekin was identified as a factor required for histone pre-mRNA processing in a genome-wide RNAi screen, along with poly(A) factors CPSF-73 and CPSF-100.[19]

How the cell assembles distinct mRNA 3' end processing complexes containing overlapping sets of components in the appropriate amounts is an open question. Symplekin is a conserved protein that contains a HEAT domain at the NH_2-terminus.[20,21] *In silico* predictions indicate that a short disordered region separates the HEAT domain from a series of predicted armadillo repeats that extend to the COOH-terminus. Proteins with these domains are frequently classified as scaffolds.[20] As a potential scaffold, Symplekin may play a critical role in assembling distinct complexes containing the CPSF complex. Symplekin and CPSF are also required for cleavage/polyadenylation directed by STAR-PAP,[22,23] as well as for cytoplasmic polyadenylation together with CPSF and cytoplasmic poly(A) polymerase.[24] Curiously, Symplekin was first discovered as a protein associated with the tight junctions of mammalian polarized epithelial cells.[25] Symplekin likely acts as a scaffold for multiple complexes primarily involved in mRNA metabolism, and whether it performs this role at the tight junction is unknown.

There are several known direct binding partners of Symplekin which have potential roles in various aspects of mRNA 3′ end formation. The N-terminal region of Symplekin interacts with Ssu72, a RNA polymerase II C-terminal domain (CTD) phospho-Ser5 phosphatase. The role of this interaction is not definitively known, but it could help link transcription and polyadenylation.[21] Symplekin likely interacts directly with CPSF during nuclear polyadenylation, and it binds tightly to CstF64 at a site that prevents subsequent binding of CstF77 and CstF50 to CstF64.[26] The Symplekin/CstF64 heterodimer may specify the interaction of the HCC with the FLASH/Lsm11 complex for histone pre-mRNA processing.[15,16] Disrupting the Symplekin/CstF64 interaction by mutations in Symplekin results in a reduced efficiency of histone pre-mRNA processing *in vivo*.[27] In addition to nuclear binding partners, Symplekin interacts with CPEB as part of its role in cytoplasmic polyadenylation[24] as well as with the dual localization factor ZONAB.[28]

The genes for the five classes of histone proteins are linked and are localized in a distinct sub-domain in the nucleus defined by the histone locus body (HLB).[29] In *Drosophila melanogaster*, which contains a tandem repeat of 100 copies of a 5kB histone repeat unit containing one copy of each of the five histone genes, there is a single HLB that is readily visualized using antibodies against Mxc (the mammalian NPAT orthologue), U7 snRNP, FLASH, or Mute, a protein of unknown activity that may function to down-regulate histone mRNA expression.[30] A likely function of the HLB is to concentrate these factors for histone mRNA biosynthesis, since they are each present at low abundance. All four of these factors are continuously present in the *Drosophila* HLB, including in cells that are not expressing histone mRNA. As mammalian cells approach S-phase, NPAT is phosphorylated by Cyclin E/Cdk2 to activate histone gene expression,[31] and *Drosophila* Mxc is phosphorylated by Cyclin E/Cdk2,[32] likely for the same function. Although U7 snRNP and FLASH are both present in the *Drosophila* HLB constitutively, it is not known whether Symplekin and other HCC components are constitutively concentrated in the HLB.

Here we have utilized a genetic system to examine how Symplekin's function in mRNA 3′ end formation contributes to development, and show that Symplekin dynamically localizes to different sites during development including the HLB and tricellular junctions.

Results

Decreased levels of Symplekin affect development

To examine the contribution of Symplekin to animal development, we characterized mutations in the *Drosophila* Symplekin (*Sym*) gene. We obtained two stocks with a P-element transposon insertion at the *Sym* locus: Sym^{NP2964}, annotated as inserted in the second exon, and $Sym^{EY20504}$, annotated as inserted in the 5′ UTR of the *Sym* gene.[33] By determining the start site of *Sym* transcription from the experimental data of Adelman and coworkers,[34] and the transposon insertion site by sequencing flanking DNA, we found that $Sym^{EY20504}$ is located in the 97 nt 5′UTR, 63 nt upstream of the translation start site (**Fig. 1A**, EY). In contrast to the original annotation, our sequencing of genomic DNA flanking Sym^{NP2964} placed the transposon in the intergenic region between *Symplekin* and the divergently transcribed *MLF1-adaptor molecule (Madm)* gene (**Fig. 1A**, NP). Sym^{NP2964} is viable and fertile in *trans* with a genomic deletion of the *Symplekin* locus ($Sym^{Df(3R)Exel7283}$; hereafter "Sym^{Df}"). $Sym^{EY20504}/Sym^{Df}$ progeny do not live past the wandering 3rd instar larval stage when Sym^{Df} is provided maternally. In contrast, when Sym^{Df} is provided paternally, 32% of the expected numbers of $Sym^{EY20504}/Sym^{Df}$ progeny survive to adulthood (**Fig. 1B**). This difference in maternal effect between Sym^{Df} and $Sym^{EY20504}$ indicates that $Sym^{EY20504}$ (hereafter, "Sym^{EY}") is a hypomorphic allele that provides some Symplekin function.

To generate additional *Sym* mutants, we mobilized the Sym^{EY} P-element and recovered and analyzed 4 alleles resulting from imprecise repair events (see Experimental Procedures for details). Three of these alleles contained internal deletions of Sym^{EY}, two of which retained a substantial amount of transposon sequence in the *Sym* 5′UTR (6,497 nts and 9,013 nts in Sym^{441} and Sym^{619},

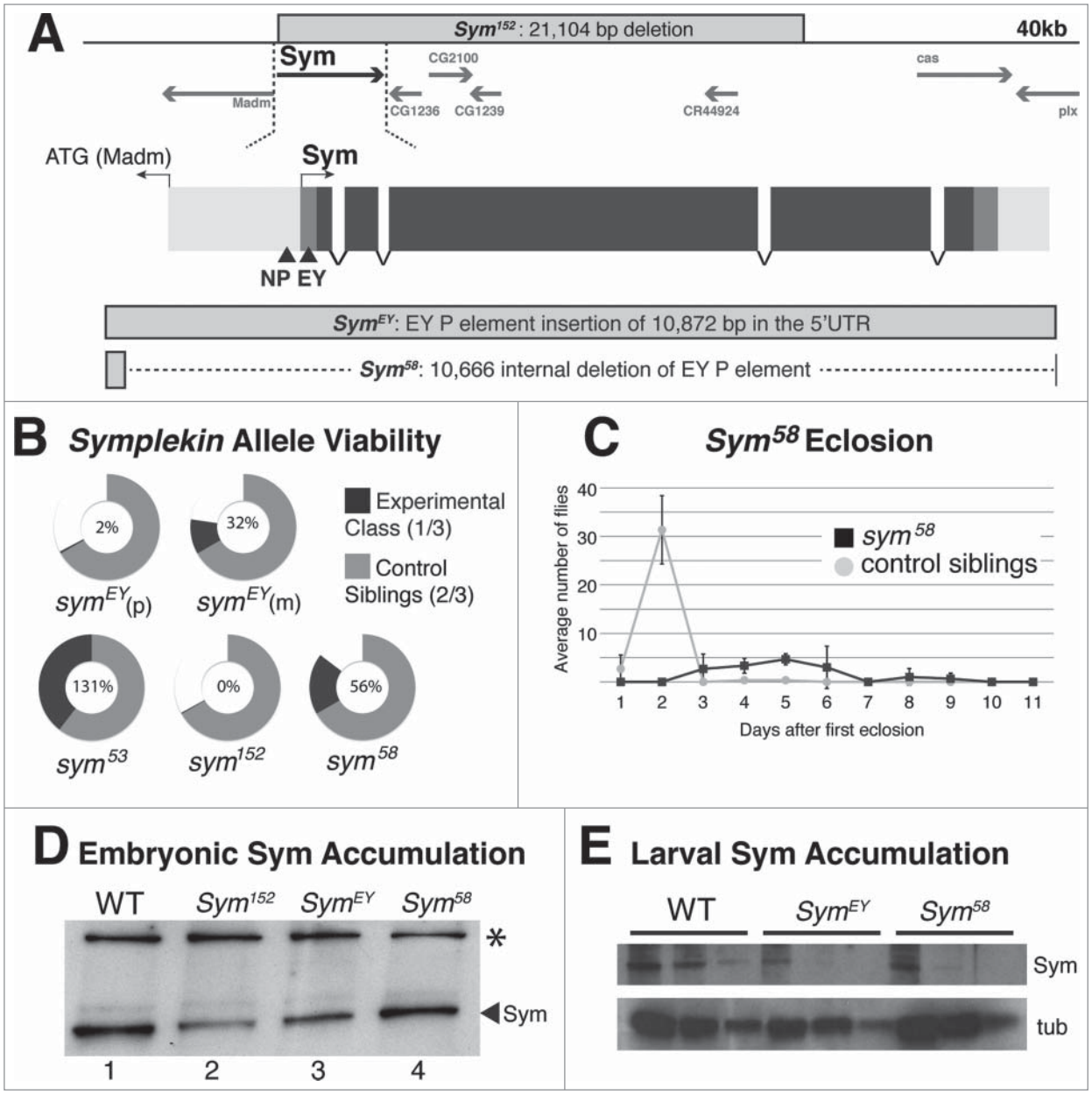

Figure 1. Developmental Analysis of Symplekin Mutants **(A).** Schematic of Symplekin locus, gene structure and mutations. Symplekin is located on the 3rd chromosome in close proximity to the essential genes madm and cas. Features of the Sym gene structure are represented by intensity of grey: intergenic (light), UTRs (medium) and ORF (dark). Transcription start sites are represented with an arrow above the gene and triangles below indicate the transposon insertion sites. Outlined boxes depict the nature of each Sym mutant. The genomic deletion in Sym^{152} is shown above the locus diagram. The EY P element inserted in Sym^{EY} and the internal deletion of the EY P element leaving 206 nts in the Sym 5'UTR resulting in Sym^{58} are represented below the Sym gene structure diagram. **(B).** Visual representation of Sym mutant viability phenotypes. Circles indicate the proportion of Sym^{allele} mutant (black) and control heterozygous sibling (grey) flies obtained in each experiment. The expected number of control siblings is 2/3. Thus, 1/3 black indicates full viability and the absence of black indicates lethality. The percentage of observed flies within the mutant class is labeled inside each circle. Note that the observed precise excision (Sym^{53}) class exceeded the expected ratio as a wild type fly is healthier than control siblings carried over a balancer chromosome. For the EY genotypes, (p) indicates a paternal and (m) indicates a maternal contribution of the transposon with the other parent providing the Df chromosome. For all of the other genotypes, the Df chromosome was maternally provided. **(C).** Visual representation of the Sym^{58} delayed eclosion phenotype. The line graph represents the daily average number of mutant and control sibling flies observed within one generation. **(D).** Symplekin protein levels in Symplekin mutant embryos. Equal amounts of total protein from 16-20 hour embryos were resolved by SDS gel electrophoresis and Symplekin detected by Western blotting. The mutant Sym^{152} (lane 2) does not express zygotic symplekin and indicates the amount of maternal Symplekin remaining at this stage. The * indicates a cross-reacting band. **(E).** Extracts from 3rd instar larvae of each genotype were analyzed by Western blotting. 3-fold dilutions of each genotype were analyzed for Symplekin (top) and the blot re-probed for tubulin (bottom).

respectively **Table S1**). These two alleles weren't considered further because they displayed the same larval lethality phenotype as Sym^{EY} (data not shown). Sym^{58} retained 206 nt of P-element sequence in the 5'UTR of *Sym*. Sym^{58}/Sym^{Df} progeny developed to adulthood (**Fig. 1B**), but these flies were male and female sterile and also developmentally delayed, eclosing 1-6 days later than siblings that contained a single wild type copy of *Sym* (**Fig. 1C**). The fourth allele, Sym^{152}, contains a complete deletion of the *Sym* coding region that extends beyond *Sym* to the 5′ control region of the downstream gene, *castor* (**Fig. 1A**). Sym^{152} causes embryonic lethality and disrupts *castor* function because it fails to complement *castor* null mutations (data not shown). We did not recover an allele that disrupts the *Sym* coding region without affecting the neighboring essential genes, *castor* and *Madm*. We isolated Sym^{53} as a precise excision event and used this allele as a wild type control in our developmental analyses to ensure that any observations were not a consequence of other lesions on the original Sym^{EY} chromosome (**Fig. 1B**).

To compare the levels of Symplekin expression from these alleles, we measured Symplekin protein in 16-20h old *Sym* mutant embryos by western blotting (**Fig. 1D**). At this stage of development, Sym^{152} and Sym^{EY} embryos have less Symplekin protein than wild type, while the amount in Sym^{58} is similar to wild type (**Fig. 1D**). The detection of Symplekin in the Sym^{152} deletion, which lacks zygotic *Symplekin* expression, indicates there is a maternal supply of Symplekin that persists until late stages of embryogenesis and likely beyond, consistent with our results from the reciprocal matings described above. Western blot analysis indicated that both mutant alleles of *Sym* expressed reduced amounts of Symplekin relative to wild type. However, these alleles expressed substantial amounts of Symplekin, with Sym^{58} expressing more Symplekin than Sym^{EY}. In Sym^{EY} mutants, Symplekin protein was reduced to ~30% of normal as judged by the zygotic expression in embryos and to ~50% of normal in Sym^{58} wandering 3rd instar larvae (**Fig. 1D, E**), consistent with allele strength as determined by the genetic results. These modest reductions in Symplekin expression indicate that relatively small changes in Symplekin protein levels have a substantial affect on development.

Pre-mRNA processing is attenuated in *Symplekin* mutants

When histone mRNA 3′ end processing is disrupted in *Drosophila* by mutation of U7 snRNP, FLASH or SLBP, longer poly-adenylated histone mRNAs accumulate because of read through transcription and subsequent utilization of cryptic poly (A) signals located downstream of the HDE in all 5 histone genes.[35-37] We analyzed histone mRNA 3′ end processing in Sym^{EY}, Sym^{58} *and* $FLASH^{LL01692}$ mutants using an S1 nuclease protection assay that distinguishes normally processed histone H2a mRNA from various mis-processed, polyadenylated H2a mRNAs as well as "read-through" transcripts that extend past the end of our probe (**Fig. 2A**). For both Sym^{EY} and Sym^{58} mutants, we analyzed total RNA from wandering 3rd instar larvae, the terminal stage of development for Sym^{EY} mutants. Because Sym^{58} mutants develop to adulthood, we also analyzed total RNA from Sym^{58} ovaries. Unlike $FLASH^{LL01692}$ or *U7 snRNP* mutants, which contain primarily misprocessed H2a mRNA,[36,37] in both Sym^{EY} and Sym^{58} we primarily found properly processed H2a mRNA (**Fig. 2A**). However, each *Sym* mutant contained small amounts of misprocessed H2a mRNA (**Fig. 2A**), indicating that histone mRNA 3' end processing was not 100% efficient. In the Sym^{58} ovaries we observed a higher level of accumulation of "read-through" RNA (**Fig. 2A**, lane 6, "R"), compared with the long polyadenylated mRNA (**Fig. 2A**, lane 6, "M") when compared to the *U7* mutant. A similar phenotype was observed in cultured S2 cells after Sym depletion and suggests that polyadenylated transcripts don't accumulate efficiently after histone pre-mRNA misprocessing due to disruption of the cleavage and polyadenylation machinery.[38]

We next asked if polyadenylation is affected in the *Sym* mutants. We analyzed two genes, *ribosomal protein L32 (Rp49)* and *ribosomal protein S2* (*sop),* that were previously shown by RT-PCR to be sensitive to disruption of the poly(A) factor, CstF77 (*Su(F)*).[39] In this assay, an amplification product is detected with primers that flank the 3' end poly(A) signals only when the pre-mRNA has not been cleaved at the normal site. Using this assay we detected misprocessed Rp49 and sop RNA in both Sym^{EY} and Sym^{58} mutants but not in wild type, demonstrating that 3' end processing of these poly(A) mRNAs is sensitive to the levels of Symplekin (**Fig. 2B**). Because a complete failure in histone pre-mRNA processing during larval stages still permits the completion of development,[40] we conclude that the lethality of the Sym^{EY} mutant and the delayed eclosion and sterility of the Sym^{58} mutant likely result from polyadenylation defects due to reduced Symplekin function and not to the small effects on histone mRNA 3' end formation that we observed in **Fig. 2A**.

Symplekin localization to the HLB during development is dynamic

Because Symplekin is required for histone pre-mRNA processing and is a component of the HCC, we asked if Symplekin is enriched in the HLB and whether its presence in the HLB changes during development. In the early syncytial cycles of *Drosophila* embryogenesis, there is very little if any transcription, and there are no HLBs. Mature HLBs containing the constitutive HLB markers, Mxc, FLASH, U7 snRNP and Mute, are formed in cycle 11, corresponding to the time when there is a large increase in the expression of zygotic histone mRNA, which continues until cycle 14[32,41] During these syncytial cycles Cyclin E/Cdk2 is constitutively active, and Mxc is phosphorylated as detected by HLB staining with the MPM-2 monoclonal antibody, which recognizes a Cyclin E/Cdk2-dependent phosphoepitope on Mxc.[32] All the HLBs are MPM-2 positive once they form at cycle 11 and remain MPM-2 positive through cycle 14.[41] We detect Symplekin accumulation in the HLBs of G2 phase of cycle 14 in gastrulating embryos (stage 6) (**Fig. 3A**). Sym positive HLBs are present in both somatic cells and the pole cells, which are germ line precursor cells that are quiescent at this time, but will re-eneter the cell cycle and proliferate during larval development.[42] In contrast, we do not detect Symplekin in the HLB of cells that have permanently exited the cell cycle, such as the highly polyploid salivary gland cells of wandering 3rd instar

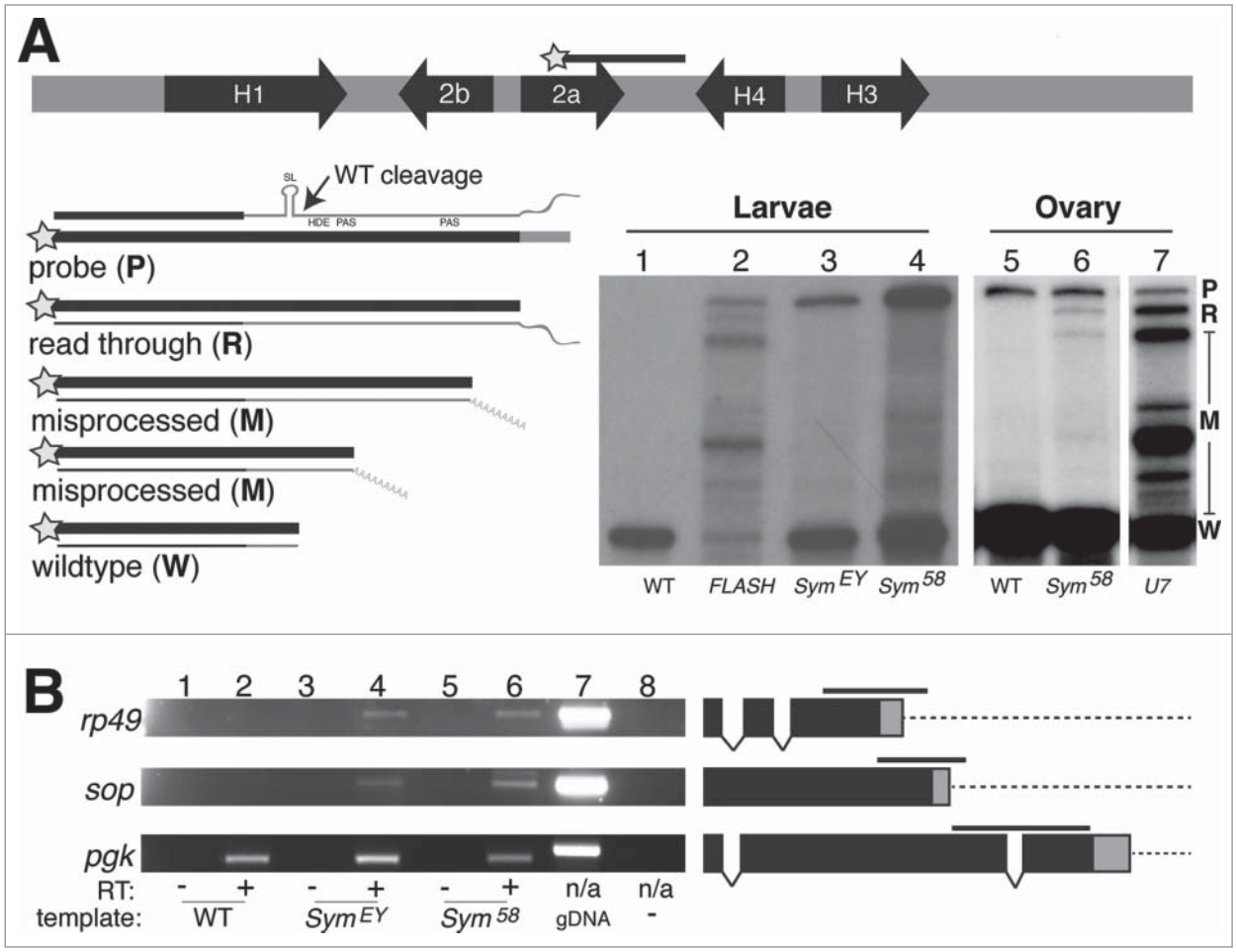

Figure 2. Depletion of Symplekin protein results in misprocessed RNA **(A).** S1 nuclease protection assay analysis of histone mRNA species in Symplekin mutants. The diagram indicates the location of the H2a probe. Total RNA extracted from wandering 3rd instar larvae or adult ovaries was hybridized with the 3′-labeled (star) DNA probe (P) and then incubated with S1 nuclease, which digests single stranded nucleic acids. The probe is complementary to the *H2a* mRNA, *H2a-H4* intergenic region up to the *H4* HDE and also contains vector sequence (3′ grey region). Properly processed histone *H2a* mRNA is cleaved between the stem loop (SL) and histone downstream element (HDE), protecting 340 bp of the DNA probe from S1 digestion (W). The *H2a* gene contains multiple cryptic poly(A) signals that are utilized in animals with disrupted histone pre-mRNA processing. These longer mis-processed polyadenylated mRNAs protect several discrete species (M). Any transcripts extending beyond the region of complementarity protect a single read-through product (R) that is distinct from undigested probe (P) and whose 3′ end(s) are likely heterogeneous. Protected probe products were resolved on an acrylamide urea gel and visualized by autoradiography. **(B).** Processing of polyadenylated mRNAs in Sym mutants was assessed by RT-PCR with primers flanking the canonical cleavage site for three mRNAs, rp49, sop and pgk. The black bar above each gene diagram represents the amplified PCR product. Black boxes represent exons, the grey box represents the 3′UTR and the dashed line represents the downstream intergenic region, which accumulates in the *Symplekin* mutant. pgk transcripts were detected in each preparation. Note that the amplified product in the *pgk* gene spans an intron that is not present in the cDNA template but is in the genomic DNA PCR control.

larvae (**Fig. 3B**). Thus, when cells are rapidly proliferating, have high Cyclin E/Cdk2 activity and are expressing histone genes (e.g. during early embryogenesis), Symplekin accumulates in the HLB. In contrast Symplekin is not concentrated in the HLB in differentiated cells that have exited the cell cycle.

Symplekin localization to follicle cell HLBs is cell cycle regulated

Two major components of the histone pre-mRNA processing system, U7 snRNP and FLASH, are constitutively present in the HLB, while a third component, SLBP, is not detected in the HLB but is present in much higher concentration throughout the nucleoplasm.[43] It is not known whether the HCC, which contains Symplekin, CstF64 and CPSF, is present in the HLB continuously in cycling cells. Because Symplekin is localized to the HLB in rapidly proliferating cells in the early embryo and not in post-mitotic salivary gland cells, we determined whether Symplekin is localized in the HLB throughout the cell cycle or perhaps only during S phase when histone genes are expressed.

To address this question we analyzed follicle cells of stage eight ovaries. These cells are endocycling, oscillating between S and G phase resulting in polyploid cells.[44,45] The cell cycle of these asynchronously replicating cells has been previously characterized, and they spend 30% of their time in S-phase and 70% in

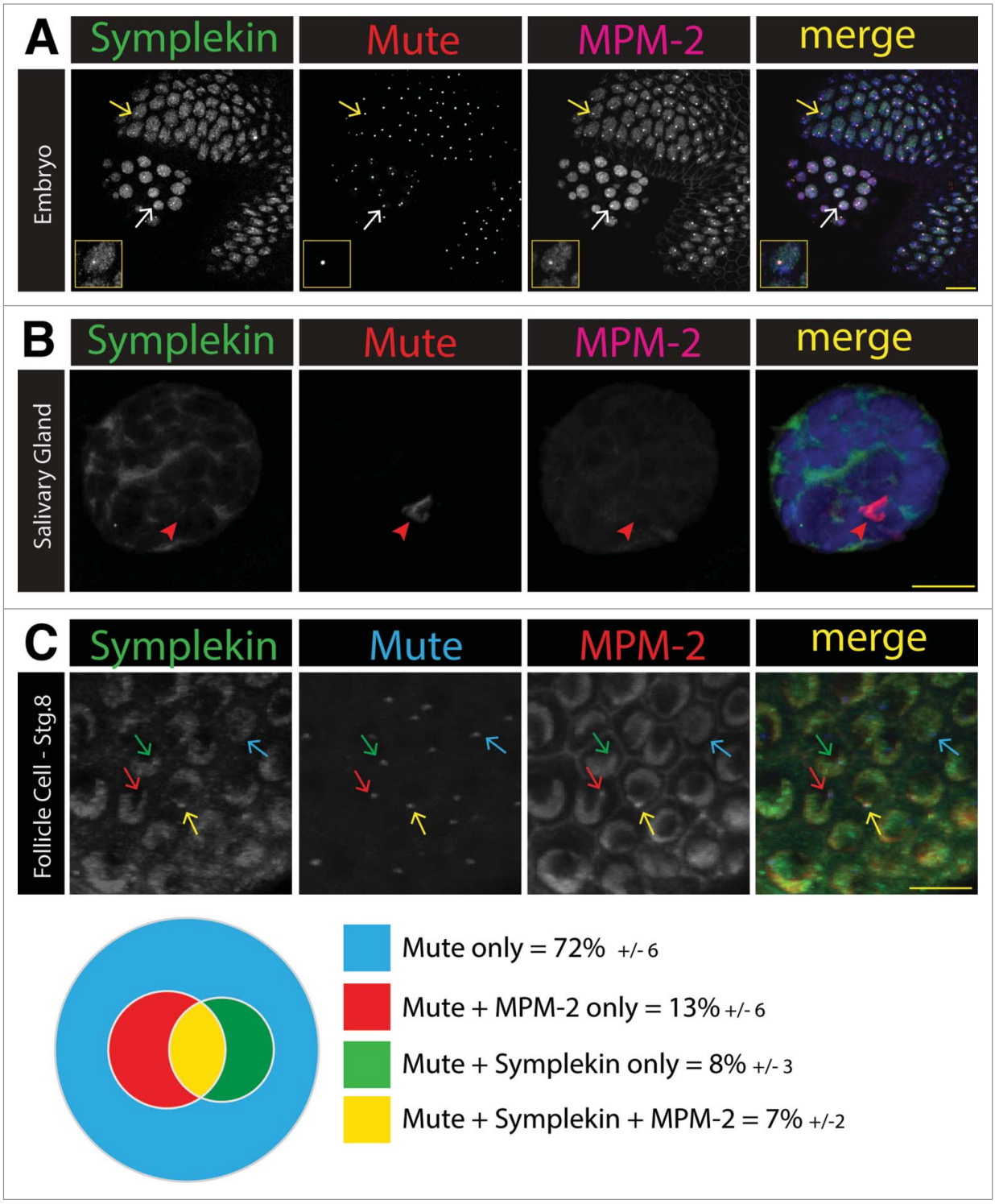

Figure 3. Symplekin concentration in the HLB is dynamic during development. **(A and B).** Projected confocal images of Symplekin localization in a syncytial embryo (A) and salivary gland nuclei (B). The presence of Symplekin in the HLB was determined by co-localization with the constitutive component Mute. Cyclin E/Cdk2 activity was monitored by staining with MPM-2, an antibody that recognizes phosphorylated epitopes in the HLB. Note that in the embryo, Sym enrichment was detected in both rapidly cycling somatic (yellow arrow) cells and germline (white arrow) cells that are not cycling. Both types of cells have MPM-2 positive HLBs whereas in the salivary gland nucleus, neither Sym nor MPM-2 signal was present in the large Mute positive HLB (red arrowhead). Scale bars = 10 microns. The inset shows a higher magnification image of a somatic cell. **(C).** Quantification of Sym HLB enrichment in endocycling stage 8 ovarian follicle cells. Ovaries were stained for Mute (blue), Sym (green) and MPM-2 (red). HLBs were defined by Mute staining, and we assessed the HLBs for co-localization with Sym and/or MPM-2. A representative projected image shows each class: Mute only (blue arrow), Mute + MPM-2 (red arrow), Mute + Symplekin (green arrow) and Mute + MPM-2 + Symplekin (yellow arrow). Quantification of individual ovaries were averaged and presented as a Venn diagram (n=6, average number of cells scored per ovary was 93 +/- 21.7). The errors represent the standard deviation.

G-phase.[46] The resulting multiple copies of the histone locus remain paired, facilitating detection of the HLB. We stained these cells with anti-Symplekin antibodies, and visualized the HLB with anti-Mute antibodies, which label the HLB throughout the cell cycle, and with MPM-2 monoclonal antibodies, which label Mxc protein in the HLB only when Cyclin E/Cdk2 is active. All the endocycling cells contained an HLB as detected by anti-Mute, and 72% stained only with anti-Mute, consistent with these representing cells in G-phase (**Fig. 3C**). The remaining 28% of cells represented three distinct populations with respect to the HLB: 13% stained only for Mute and MPM-2, 8% stained only for Mute and Symplekin, and 7% stained for Mute, MPM-2 and Symplekin (**Fig. 3C**). Because phosphorylated Mxc (i.e. MPM-2) is present in 20% (13% MPM-2/Mute alone + 7% all three) of the HLBs and Symplekin is concentrated in 15% of the HLBs (8% Sym/Mute alone + 7% all three), these results suggest that neither MPM-2 nor Symplekin staining encompasses all of S phase. Cyclin E/Cdk2 is activated just prior to S-phase and its activity persists throughout much but not all of S-phase. MPM-2 likely stains some cells that haven't yet entered S-phase, and may not stain late S-phase cells. Thus it won't perfectly track active histone mRNA synthesis throughout S-phase. These data demonstrate that Symplekin is not a constitutive component of the HLB, but it likely cycles, and is concentrated in the HLB during at least part of S-phase.

Symplekin localizes to tricellular junctions in stage 10B follicle cells

Symplekin is present in the nucleoplasm of follicle cells, which produce large amounts of mRNA and protein for eggshell production and vitellogenesis.[47] Additionally we detected Symplekin accumulation at the follicle cell cortex during stage 10B, specifically within a region of the cortex corresponding to the tricellular junction[48,49] (**Fig. 4A**). We further characterized this striking localization by structured illumination fluorescence microscopy (**Fig. 4B**, Supplemental movie 1) and confirmed that Symplekin localized to the tri-cellular junction of stage 10B follicle cells by expressing ectopic HA tagged Symplekin and visualizing it with anti-HA antibodies (**Fig. 4C**). We also used an antibody against gliotactin, an integral membrane protein that is found at tricellular junctions[48,50] to confirm that this localization was actually at the tricellular junction. Anti-gliotactin stains the tricellular junction in the follicle cells. Symplekin colocalizes to the same region as gliotactin, consistent with Symplekin being recruited to the tricellular junction, likely as part of a much larger complex (**Fig. 4D**).

Because Symplekin is involved in cytoplasmic polyadenylation, we tested whether CPSF-73, another component of the cytoplasmic polyadenylation machinery, also localized to tricellular junctions. We stained ovaries with antibodies against CPSF-73 and CstF64, a component of CstF which is not involved in cytoplasmic polyadenylation. CPSF-73 was concentrated at the tricellular junctions in stage 10B follicle cells (**Fig. 4E**), as well as in the nucleoplasm. CstF64 was not concentrated at the tricellular junctions but was only detected in the nucleoplasm (**Fig. 4F**).

Symplekin was first described as a protein that localized to tight junctions in mammalian cells.[25] Symplekin was later characterized as a component of the mRNA 3′ end formation machinery.[18,19,24,26,51] Studies of a mammalian intestinal epithelial cell line, HT-29, showed that Symplekin and the Y box protein ZONAB, co-localize at tight junctions as well as being found in the nucleoplasm.[28] This study also showed a direct interaction between recombinant Symplekin and ZONAB, whose closest homologue in *Drosophila* is the Y box protein, ypsilon schachtel (Yps) (**Fig. 4I**).

Yps interacts with RNA trafficking proteins and is a component of the oskar mRNP, although its precise role in RNA metabolism is not clear.[52,53] Like Symplekin, cytoplasmic Yps is enriched at the tricellular junctions of stage 10B follicle cells (**Fig. 4G**), further suggesting that mRNP(s) containing cytoplasmic polyadenylation factors accumulate at tricellular junctions. Yps is also present in the cytoplasm but is not detected in the nucleoplasm. To test if Symplekin localization depends on Yps, we stained $yps^{JM2/Df(3L)BK9}$ mutant ovaries with anti-Symplekin antibodies. Symplekin did not localize to the tricellular junction in stage 10B *yps* mutant follicle cells, but instead was dispersed in the cytoplasm in addition to the nucleoplasm (**Fig. 4H**). We conclude that Yps is required for Symplekin localization to the tricellular junction, but that the accumulation of cytoplasmic Symplekin in stage 10B follicle cells occurs independently of Yps.

Taken together these data suggest that Symplekin is present at tricellular junctions as part of a complex involved in cytoplasmic RNA metabolism. In support of this conclusion, an earlier study demonstrated that at Stage 10B of follicle cell development, a set of mRNAs encoding integral membrane proteins are concentrated and translated at the tricellular junctions,[54] providing potential substrates for the cytoplasmic Symplekin complex.

Discussion

Our genetic data clearly demonstrate that Symplekin is essential for development and that reducing the concentration of Symplekin affects the efficiency of mRNA 3' end formation. A small reduction in the amount of Symplekin has severe effects on development, in a concentration-dependent manner, consistent with Symplekin playing multiple roles *in vivo*. Symplekin participates in multiple aspects of RNA metabolism in metazoans including canonical and STAR-PAP-mediated cleavage-polyadenylation in the nucleus, cytoplasmic polyadenylation, and histone pre-mRNA processing. In each case Symplekin acts as part of a multi-protein complex, likely performing a scaffolding role. How the cell distributes a single protein among a variety of different cellular complexes is not clear. As a potential interface between specialized *trans* factors and general components of 3′ end processing machinery, Symplekin may help determine the composition of each of these multi-protein complexes by binding specific *trans* factors to assemble the appropriate complex at the appropriate site for each 3′ end processing reaction (**Fig. 5**).

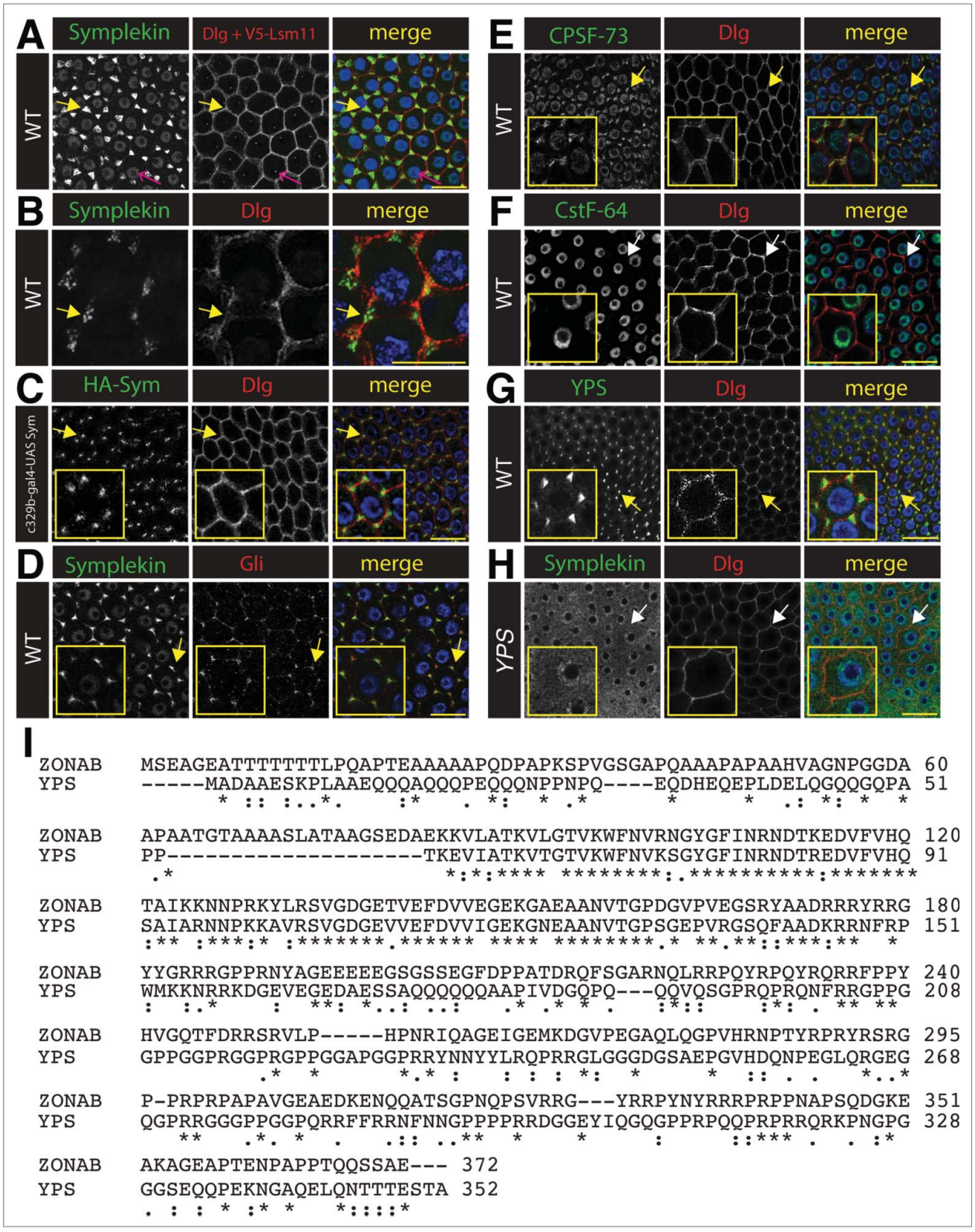

Figure 4. For figure legend, see page 621.

Assembling Symplekin into the histone pre-mRNA processing complex

Symplekin participates in two distinct mRNA 3′ end-processing pathways in the nucleus, cleavage of histone pre-mRNAs and cleavage/polyadenylation of all other mRNAs. Because of the very small fraction of polyadenylation factors present in the HLB, formation of the active U7 snRNP does not result in the loss of significant cleavage/polyadenylation activity. In nuclear extracts from *Drosophila* or mammalian cells <1% of the polyadenylation factors are present in the HCC bound to U7 snRNP.[15,16] 99% of the Symplekin is likely dedicated to cleavage/polyadenylation. In nuclear extracts Symplekin can readily exchange between a polyadenylation complex and the HCC, since addition of the FLASH/Lsm11 complex to these extracts results in up to 40% of the Symplekin and CPSF being assembled into the HCC.[16] Thus, the Lsm11/FLASH complex can drive assembly of the HCC, and the amount of the FLASH/Lsm11 complex limits how much of the HCC can form. The current evidence suggests that the Symplekin/CstF64 heterodimer is the form of Symplekin incorporated into the HCC, which then binds the CPSF complex,[16,26,27] as well as FLASH/Lsm11.[16] The amount of U7 snRNA (and hence the amount of Lsm11 in the U7 snRNP) or the amount of FLASH, whichever is lower, determines the maximal amount of the HCC that can be present at any particular time.

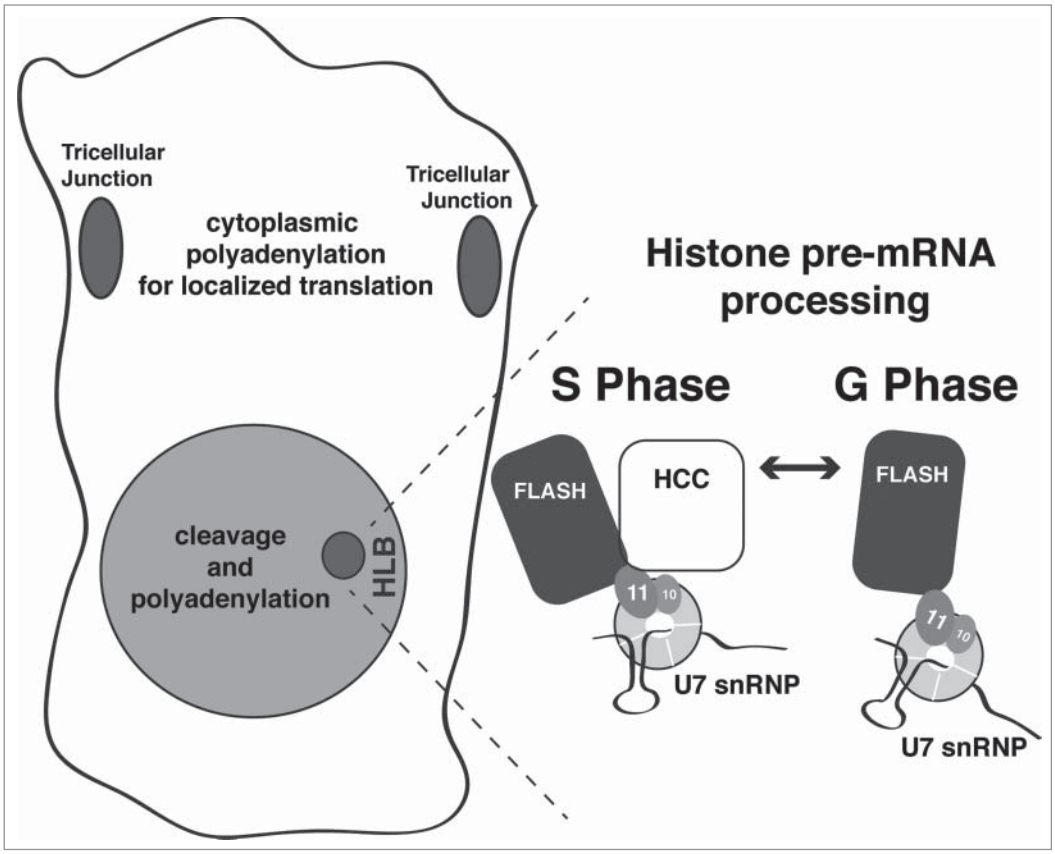

Figure 5. Summary of Symplekin subcellular localization and model of HLB dynamics. Symplekin localization observed in this study is summarized in the cell drawn on the left. Grey shading represents the diffuse Symplekin accumulation in the nucleus, consistent with its role in cleavage-polyadenylation. The darker grey indicates sites of Symplekin concentration: in the tricellular junctions, where it likely participates in cytoplasmic polyadenylation leading to localized translation; and in the HLB, where it is required for histone mRNA biosynthesis. The expanded HLB depicts fluctuating concentration of Sym during the cell cycle. During S phase or when there is high activity of Cyclin E/Cdk2, Symplekin (and likely the HCC) localizes to the HLB and interacts with a unique surface generated by an interaction between FLASH and the U7 snRNP component Lsm11, creating the active form of U7 snRNP.

There are three potential states of the U7 snRNP: the core U7 snRNP, which can bind to histone pre-mRNA, the U7 snRNP bound to FLASH, and the active U7 snRNP containing the HCC bound to the Lsm11/FLASH complex.[15] U7 snRNP and FLASH are constitutive components of the HLB, but Symplekin is not

Figure 4 (See previous page). Symplekin localizes to the tri-cellular junction in stage 10B ovary follicle cells. **(A–D).** Projected confocal images of the localization of Symplekin in stage 10B ovarian follicle at the tricellular junctions. (**A**) A V5-tagged Lsm11 replacement strain that has a wild-type phenotype.[37] Note that these cells are stained with anti-Dlg and anti-V5 antibodies in the same channel to simultaneously identify cell boundaries (yellow arrow) and V5-Lsm11 in the HLB (pink arrow). (B) Visualization of Symplekin and Discs large in wild type stage 10B ovarian follicle cells by structured illumination fluorescence microscopy. Note that Symplekin accumulates at the cell cortex where three cells come together (yellow arrow). (**C**) Follicle cells expressing HA tagged-Sym stained with anti-HA antibodies. (**D**) Wild type follicle cells stained with anti-Sym and anti-Gliotactin, a tricellular junction marker. **(E–F).** Localization of additional RNA processing factors in stage 10B ovarian follicle cells. Wild type follicle cells stained with anti-CPSF73 and anti-Dlg antibodies (E) or anti-CstF64 and anti-Dlg (F). Note that components of the cytoplasmic polyadenylation complex (Sym and CPSF-73) localize to the tri-cellular junction (yellow arrow), whereas CstF-64 does not (white arrow).**(G–H).** Projected confocal images representing the relationship between Sym and RNA binding protein *yps* in stage 10B ovarian follicle cells. Wild-type cells were stained with Yps and Dlg (G). Yps is enriched at the tricellular junctions (yellow arrow). $yps^{JM2/Df(3L)BK9}$ mutant cells were stained for Sym and Dlg (H). In the *yps* mutant Sym is diffuse in the cytoplasm. Yellow bars = 10 microns. Arrow indicates magnified cell shown in inset in panels C-H (yellow box) **(I)**. Alignment (ClustalW2) of the amino sequences of human ZONAB and *Drosophila yps*.

present in the HLB in cells that have exited the cell cycle, suggesting that the HCC normally concentrates in the HLB on the U7 snRNP/FLASH complex to activate histone pre-mRNA processing. Thus, one way to regulate processing would be to regulate the binding of the HCC to the U7 snRNP (**Fig. 5**), possibly as a result of activation of Cyclin E/Cdk2. We found that Symplekin is present in the HLB in early embryos when Cyclin E/Cdk2 is active, including the pole cells even when they are not replicating, indicating that ongoing histone gene transcription is not essential for Symplekin recruitment. An attractive scenario is that the HCC is present in the HLB throughout much of S phase allowing efficient expression of histone mRNA. At the end of S-phase the U7 snRNP may be inactivated by loss of the HCC (**Fig. 5**). This model fits our observation that Symplekin does not concentrate in the HLB of postmitotic cells, and that Symplekin localization in the HLB cycles in endoreduplicating follicle cells. Since Symplekin and the HCC complex have the potential to convert U7 snRNP, which is constitutively present in the HLB, from an inactive form to an active form, localization of Symplekin to the HLB is an essential step for activating histone mRNA biosynthesis,

What is the role of symplekin at the tricellular junction?

In stage 10B follicle cells, in contrast to younger endoreduplicating follicle cells, a substantial fraction of Symplekin is present in the cytoplasm and accumulates at the tricellular junctions together with CPSF-73 and Yps but not CstF64. The follicle cells produce proteins needed for egg development, including the yolk and eggshell, and follicle cell movement confer the characteristic shape to the oocyte.[55] At stage 10B, when follicle cells undergo centripetal migration to encapsulate the expanding oocyte, a subset of mRNAs including dGRASP are localized to and translated at the tricellular junction (alternately termed zone of contact).[54] At least 5 mRNAs encoding integral membrane or secreted proteins are localized at this time. Temporal and localized control of dGRASP protein expression results in non-canonical secretion of integrin αPS1 to maintain epithelial integrity and adhesion to the extracellular matrix.[54] Thus Symplekin accumulation at the junction during this specific stage of oogenesis likely reflects the localization of a specific subset of mRNAs and the cytoplasmic polyadenylation machinery, of which Symplekin and CPSF-73 are components, resulting in regulated translation of a number of mRNAs.

Yps is part of the mRNP that traffics *osk* mRNA along microtubules and has been implicated in translational repression of *oskar* mRNA.[52,53] Our data show that Symplekin localization to the junction requires Yps suggesting that Yps could contribute to regulation of dGRASP both by promoting localization of the mRNA and directly interacting with the cytoplasmic polyadenylation machinery at the junction to enhance translation. ZONAB, the closest Yps homolog in mammals, interacts with Symplekin at tight junctions in mammalian cells suggesting that this strategy for synthesis of proteins at cell junctions has been conserved in evolution.[28] The translation of at least one protein, ZO-1, which binds ZONAB, is regulated by cytoplasmic polyadenylation at the mammalian cell junctions.[56]

Future combined genetic and cell biological approaches will help reveal the molecular details of how Symplekin assembles into different complexes in distinct subcellular compartments to facilitate its multiple functional roles in RNA metabolism.

Materials and Methods

***Drosophila* genetics**

$Sym^{EY20504}$ was obtained from the Bloomington Stock Center and Sym^{NP2964} from the Drosophila Genetic Resource Center. To generate additional *Sym* mutant alleles, excisions of *EY20504* were recovered over Tm3 as white eyed male progeny from w^{1118}*; P [EY20504]*ry^{506}*, Sb, P[ry* D2-3]* fathers. These single males were crossed to w^{1118}*;Df(3R)7283 /Tm3, Ser, e, p[twi-GFP]* females. Males that failed to complement lethality were next crossed to y^{1}*, w*; P[lacW]*cas^{jC2}*/Tm3, Sb and* w^{1118}*;P[EP]*$Madm^{EP3137}$*/TM6B,* Tb^{1} to ensure that the excision did not disrupt vicinal, essential genes. Excision events were also characterized by PCR (see below). Of the 1,050 single males tested, we focused on four mutant excision events. Three were internal deletions of *EY20504,* and the other was a deletion that extended to the *cas* promoter. Breakpoint sequences are presented in **Table S1**. $FLASH^{LL01602}$ was previously characterized,[37] as was the $Lsm11^{c02047}$, P[V5-Lsm11+] line used for staining.[40] UAS-Sym-HA was generated by fC31 mediated integration at the VK0033 landing site of a pUASg-HA plasmid containing the full length *Sym* coding sequence. The C329b-Gal4 driver was obtained from the Bloomington Stock Center. The yps^{JM2} *and Df (3L)BK9* mutant flies were obtained from the Wilhelm Lab. WT indicates w^{1118}.

***Sym* allele analysis**

The *EY20504* and *NP2964* insertion sites were determined by PCR. All primer sequences are documented in Table S2. DNA was prepared by single fly squash prep (10 mM Tris pH 8.2, 25 mM NaCl, 1mM EDTA, 200 μg/mL Proteinase K) or by the protocol provided by the Berkeley Drosophila Genome Project. 1 μL of either prep was used for each PCR. Primers pOUT and either CG2097 DNA 1F or CG2097 DNA 1R were used for each PCR reaction to determine the insertion site of each transposon, as well as to screen for excision of the EY20504 transposon. PCR was also used to identify the breakpoints of the four excision alleles. CG2097 DNA 1F and R were used to identify the lesion in Sym^{58} as well as the precise excision in Sym^{53}. Primers pairs throughout the EY element are listed and were used to determine the Sym^{441} and Sym^{619} sequence. The primer pair 152 breakpoint primer F and 152 breakpoint primer R flank repaired DNA in Sym^{152}. Mapping Sym^{152} required isolation of homozygous embryos, as the endogenous locus on the balancer interfered with the PCR. Primer sequences are summarized in Table S2.

Western blot

16-20h embryos homozygous for WT, Sym^{152}, Sym^{EY}, *or* Sym^{58} chromosomes were isolated by lack of GFP expression with a COPAS-Select Embryo Sorter (Union Biometrica). 100 embryos per genotype were boiled in SDS loading buffer followed by shearing 25 times with a 27.5 gauge needle. 7.5 embryos per genotype were resolved on a 10% gel by SDS-

PAGE. Alternatively ten mutant larvae of each genotype were identified by lack of GFP and dissected brains, larval imaginal discs and salivary glands were boiled in 100 μL SDS loading buffer and sheared as described above with a 27.5 gauge needle and 30 μL of each sample was resolved on a 10% gel by SDS-PAGE. After transfer to a PVDF membrane, the blot was probed for Symplekin with an anti-rabbit Symplekin antibody (1:1000),[38] and donkey anti-rabbit HRP (1:10,000; GE Healthcare). After exposure of the blot with ECL Prime (embryo) (Amersham), or SuperSignal West Dura Chemiluminescent Substrate (larvae) (Pierce) signal to film, the larval blot was probed for tubulin with an anti-α-tubulin antibody (1:30,000; Sigma), ECL donkey anti-mouse HRP (1:10,000; GE Healthcare) and Super-Signal West Pico Chemiluminescent Substrate (Pierce) to capture signal from the loading control on film. The relative amounts of Symplekin in Sym^{EY} and Sym^{58} mutant animals were determined by gel analysis of film exposures with Image J software.

RT-PCR

Total RNA was extracted from whole control and mutant wandering 3rd instar larvae that were identified by lack of GFP with Trizol Reagent (Invitrogen). 2 μg of total RNA was treated with DNase (Fermentas). Samples were divided in half, and a master mix of all of the reagents for reverse transcriptase (except the RT enzyme) was added to each sample (cDNA Synthesis Kit, Fermentas). Reverse transcriptase was added to one sample per genotype. After cDNA synthesis, 1:5 dilutions of sample were used for each 25 μL PCR reaction. Genomic DNA prepared from WT larvae (as described above) was used as a positive control for the PCR reaction. Indicated primers were used with TAQ DNA Polymerase (NEB), resolved on a 2% agarose gel and visualized by ethidium bromide staining. The sequences are included in Table S2.

S1 protection assay

5 μg of RNA for each genotype was used for the S1 nuclease protection assay. The probe and method used have been previously described.[57] Briefly, the probe was generated by end labeling a BspEI cut *H2a* DNA with α-^{32}P-dCTP and Klenow Polymerase (NEB). After release from the TOPO TA vector (Invitrogen) by digestion with HindIII (NEB), the probe was gel purified and hybridized to total RNA from the indicated genotype. Following digestion by S1 nuclease (Promega), protected DNA fragments were resolved on a 6% acrylamide-7M urea gel and visualized by autoradiography.

Immunofluorescence

WT embryos were dechorionated, fixed in a 1:1 mixture of 7% formaldehyde/heptane for 25 min, and incubated with primary and secondary antibodies overnight at 4°C and for 1 h at 25°C, respectively. Salivary glands were dissected in PBS + 0.1% TritonX-100 and ovaries were dissected in Grace's medium (GIBCO). Both tissues were fixed in 7% formaldehyde for 25 min and permeabilized in a mixture of PBS and 0.2% Tween for 15 min. Samples were blocked for 30 min with Enhancer (Invitrogen) and incubated with primary and secondary antibodies overnight at 4 C and for 1 h at 25 C, respectively. Primary antibodies used were polyclonal rabbit anti-Symplekin (1:1000), polyclonal rabbit anti-YPS (1:1000), polyclonal rabbit anti-CPSF73 (1:1000), polyclonal guinea pig anti-Mute (1:5000), monoclonal mouse anti-MPM2 (Millipore), monoclonal mouse anti-Discs Large (1:1000, Developmental Studies Hybridoma Bank), monoclonal mouse anti-Gliotactin (1:300), monoclonal mouse anti-HA (1:1000; UNC Hybridoma) and monoclonal mouse anti-V5 (1:1000; Invitrogen). Secondary antibodies used were goat anti-mouse IgG-Cy3 (Jackson Immuno Research Laboratories), goat anti-guinea pig IgG-Cy5 (Jackson Immuno Research Laboratories) and goat anti-rabbit Alexafluor 488 (Invitrogen). DNA was detected by staining samples with 4,6-diamidino-2-phenylindole (DAPI) (1:1000 of 1 mg/mL stock, Dako North America) for 1 min. Images, with the exception of panel 4B, were obtained on a Zeiss 510 or 710 Confocal Microscope using a 40x objective lens. Images were prepared with Lsm Software (Zeiss) and Photoshop (Adobe). The SIM structured illumination fluorescence microscopy images presented in panel 4B were obtained with a DeltaVision OMX (GE Healthcare) imaging system. Images were collected with a 60X oil objective [Olympus PlanApo 60X, 1.42NA]. The OMX images were processed with the Imaris software and PhotoShop. Images shown are max intensity projections of several z-slices. The reconstructed 3D image (sup. movie 1) was generated by the OMX software (softWoRx).

Disclosure of Potential Conflicts of Interest

No potential conflicts of interest were disclosed.

Acknowledgments

We thank James Wilhelm for the YPS antibody and mutant flies, Vanessa Auld for the Gliotactin antibody, Johannes Bischof for the pUASg-HA attB vector and Alan Fanning for helpful discussions.

Funding

This work was supported by NIH Grant GM58921 to WFM and RJD.

Supplemental Material

Supplemental data for this article can be accessed on the publisher's website: http://www.tandfonline.com/kncl

References

1. Moore MJ, Proudfoot NJ. Pre-mRNA processing reaches back to transcription and ahead to translation. Cell 2009; 136:688-700; PMID:19239889; http://dx.doi.org/10.1016/j.cell.2009.02.001
2. Marzluff WF, Wagner EJ, Duronio RJ. Metabolism and regulation of canonical histone mRNAs: life without a poly(A) tail. Nat Rev Genet 2008; 9:843-54; PMID:18927579; http://dx.doi.org/10.1038/nrg2438; 10.1038/nrg2438
3. Proudfoot NJ. Ending the message: Poly(A) signals then and now. Genes Dev 2011; 25:1770-82; PMID:21896654; http://dx.doi.org/10.1101/gad.17268411

4. Mandel CR, Bai Y, Tong L. Protein factors in pre-mRNA 3'-end processing. Cell Mol Life Sci 2008; 65:1099-122; PMID:18158581; http://dx.doi.org/10.1007/s00018-007-7474-3
5. Mandel CR, Kaneko S, Zhang H, Gebauer D, Vethantham V, Manley JL, Tong L. Polyadenylation factor CPSF-73 is the pre-mRNA 3'-end-processing endonuclease. Nature 2006; 444:953-6; PMID:17128255; http://dx.doi.org/10.1038/nature05363
6. Martin F, Schaller A, Eglite S, Schumperli D, Muller B. The gene for histone RNA hairpin binding protein is located on human chromosome 4 and encodes a novel type of RNA binding protein. EMBO J 1997; 16:769-78; PMID:9049306; http://dx.doi.org/10.1093/emboj/16.4.769
7. Mowry KL, Steitz JA. Identification of the human U7 snRNP as one of several factors involved in the 3′ end maturation of histone premessenger RNA's. Science 1987; 238:1682-7; PMID:2825355
8. Schaufele F, Gilmartin GM, Bannwarth W, Birnstiel ML. Compensatory mutations suggest that base-pairing with a small nuclear RNA is required to form the 3′ end of H3 messenger RNA. Nature 1986; 323:777-81; PMID:3022153; http://dx.doi.org/10.1038/323777a0
9. Wang ZF, Whitfield ML, Ingledue TC,3rd, Dominski Z, Marzluff WF. The protein that binds the 3′ end of histone mRNA: A novel RNA-binding protein required for histone pre-mRNA processing. Genes Dev 1996; 10:3028-40; PMID:8957003
10. Pillai RS, Will CL, Luhrmann R, Schumperli D, Muller B. Purified U7 snRNPs lack the sm proteins D1 and D2 but contain Lsm10, a new 14 kDa sm D1-like protein. EMBO J 2001; 20:5470-9; PMID:11574479; http://dx.doi.org/10.1093/emboj/20.19.5470
11. Pillai RS, Grimmler M, Meister G, Will CL, Luhrmann R, Fischer U, Schumperli D. Unique sm core structure of U7 snRNPs: Assembly by a specialized SMN complex and the role of a new component, Lsm11, in histone RNA processing. Genes Dev 2003; 17:2321-33; PMID:12975319; http://dx.doi.org/10.1101/gad.274403
12. Burch BD, Godfrey AC, Gasdaska PY, Salzler HR, Duronio RJ, Marzluff WF, Dominski Z. Interaction between FLASH and Lsm11 is essential for histone pre-mRNA processing in vivo in drosophila. RNA 2011; 17:1132-47; PMID:21525146; http://dx.doi.org/10.1261/rna.2566811
13. Yang XC, Burch BD, Yan Y, Marzluff WF, Dominski Z. FLASH, a proapoptotic protein involved in activation of caspase-8, is essential for 3′ end processing of histone pre-mRNAs. Mol Cell 2009; 36:267-78; PMID:19854135; http://dx.doi.org/10.1016/j.molcel.2009.08.016
14. Dominski Z, Yang XC, Marzluff WF. The polyadenylation factor CPSF-73 is involved in histone-pre-mRNA processing. Cell 2005; 123:37-48; PMID:16213211; http://dx.doi.org/10.1016/j.cell.2005.08.002
15. Sabath I, Skrajna A, Yang XC, Dadlez M, Marzluff WF, Dominski Z. 3'-end processing of histone pre-mRNAs in drosophila: U7 snRNP is associated with FLASH and polyadenylation factors. RNA 2013; PMID:24145821; http://dx.doi.org/10.1261/rna.040360.113
16. Yang XC, Sabath I, Debski J, Kaus-Drobek M, Dadlez M, Marzluff WF, Dominski Z. A complex containing the CPSF73 endonuclease and other polyadenylation factors associates with U7 snRNP and is recruited to histone pre-mRNA for 3'-end processing. Mol Cell Biol 2013; 33:28-37; PMID:23071092; http://dx.doi.org/10.1128/MCB.00653-12
17. Gick O, Kramer A, Vasserot A, Birnstiel ML. Heat-labile regulatory factor is required for 3' processing of histone precursor mRNAs. Proc Natl Acad Sci U S A 1987; 84:8937-40; PMID:2962194
18. Kolev NG, Steitz JA. Symplekin and multiple other polyadenylation factors participate in 3′-end maturation of histone mRNAs. Genes Dev 2005; 19:2583-92; PMID:16230528; http://dx.doi.org/10.1101/gad.1371105
19. Wagner EJ, Burch BD, Godfrey AC, Salzler HR, Duronio RJ, Marzluff WF. A genome-wide RNA interference screen reveals that variant histones are necessary for replication-dependent histone pre-mRNA processing. Mol Cell 2007; 28:692-9; PMID:18042462; http://dx.doi.org/10.1016/j.molcel.2007.10.009
20. Kennedy SA, Frazier ML, Steiniger M, Mast AM, Marzluff WF, Redinbo MR. Crystal structure of the HEAT domain from the pre-mRNA processing factor symplekin. J Mol Biol 2009; 392:115-28; PMID:19576221; http://dx.doi.org/10.1016/j.jmb.2009.06.062
21. Xiang K, Nagaike T, Xiang S, Kilic T, Beh MM, Manley JL, Tong L. Crystal structure of the human symplekin-Ssu72-CTD phosphopeptide complex. Nature 2010; 467:729-33; PMID:20861839; http://dx.doi.org/10.1038/nature09391; 10.1038/nature09391
22. Laishram RS, Anderson RA. The poly A polymerase star-PAP controls 3′-end cleavage by promoting CPSF interaction and specificity toward the pre-mRNA. EMBO J 2010; 29:4132-45; PMID:21102410; http://dx.doi.org/10.1038/emboj.2010.287
23. Mellman DL, Gonzales ML, Song C, Barlow CA, Wang P, Kendziorski C, Anderson RA. A PtdIns4,5P2-regulated nuclear poly(A) polymerase controls expression of select mRNAs. Nature 2008; 451:1013-7; PMID:18288197; http://dx.doi.org/10.1038/nature06666
24. Barnard DC, Ryan K, Manley JL, Richter JD. Symplekin and xGLD-2 are required for CPEB-mediated cytoplasmic polyadenylation. Cell 2004; 119:641-51; PMID:15550246; http://dx.doi.org/10.1016/j.cell.2004.10.029
25. Keon BH, Schafer S, Kuhn C, Grund C, Franke WW. Symplekin, a novel type of tight junction plaque protein. J Cell Biol 1996; 134:1003-18; PMID:8769423
26. Takagaki Y, Manley JL. Complex protein interactions within the human polyadenylation machinery identify a novel component. Mol Cell Biol 2000; 20:1515-25; PMID:10669729
27. Ruepp MD, Schweingruber C, Kleinschmidt N, Schumperli D. Interactions of CstF-64, CstF-77, and symplekin: Implications on localisation and function. Mol Biol Cell 2011; 22:91-104; PMID:21119002; http://dx.doi.org/10.1091/mbc.E10-06-0543
28. Kavanagh E, Buchert M, Tsapara A, Choquet A, Balda MS, Hollande F, Matter K. Functional interaction between the ZO-1-interacting transcription factor ZONAB/DbpA and the RNA processing factor symplekin. J Cell Sci 2006; 119:5098-105; PMID:17158914; http://dx.doi.org/10.1242/jcs.03297
29. Liu JL, Murphy C, Buszczak M, Clatterbuck S, Goodman R, Gall JG. The drosophila melanogaster cajal body. J Cell Biol 2006; 172:875-84; PMID:16533947; http://dx.doi.org/10.1083/jcb.200511038
30. Bulchand S, Menon SD, George SE, Chia W. Muscle wasted: A novel component of the drosophila histone locus body required for muscle integrity. J Cell Sci 2010; 123:2697-707; PMID:20647374; http://dx.doi.org/10.1242/jcs.063172
31. Ye X, Wei Y, Nalepa G, Harper JW. The cyclin E/Cdk2 substrate p220(NPAT) is required for S-phase entry, histone gene expression, and cajal body maintenance in human somatic cells. Mol Cell Biol 2003; 23:8586-600; PMID:14612403
32. White AE, Burch BD, Yang XC, Gasdaska PY, Dominski Z, Marzluff WF, Duronio RJ. Drosophila histone locus bodies form by hierarchical recruitment of components. J Cell Biol 2011; 193:677-94; PMID:21576393; http://dx.doi.org/10.1083/jcb.201012077
33. St Pierre SE, Ponting L, Stefancsik R, McQuilton P, FlyBase Consortium. FlyBase 102–advanced approaches to interrogating FlyBase. Nucleic Acids Res 2014; 42:D780-8; PMID:24234449; http://dx.doi.org/10.1093/nar/gkt1092 [doi]
34. Nechaev S, Fargo DC, dos Santos G, Liu L, Gao Y, Adelman K. Global analysis of short RNAs reveals widespread promoter-proximal stalling and arrest of pol II in drosophila. Science 2010; 327:335-8; PMID:20007866; http://dx.doi.org/10.1126/science.1181421
35. Sullivan E, Santiago C, Parker ED, Dominski Z, Yang X, Lanzotti DJ, Ingledue TC, Marzluff WF, Duronio RJ. Drosophila stem loop binding protein coordinates accumulation of mature histone mRNA with cell cycle progression. Genes Dev 2001; 15:173-87; PMID:11157774
36. Godfrey AC, Kupsco JM, Burch BD, Zimmerman RM, Dominski Z, Marzluff WF, Duronio RJ. U7 snRNA mutations in drosophila block histone pre-mRNA processing and disrupt oogenesis. RNA 2006; 12:396-409; PMID:16495235; http://dx.doi.org/12/3/396 [pii]
37. Rajendra TK, Praveen K, Matera AG. Genetic analysis of nuclear bodies: From nondeterministic chaos to deterministic order. Cold Spring Harb Symp Quant Biol 2010; 75:365-74; PMID:21467138; http://dx.doi.org/10.1101/sqb.2010.75.043
38. Sullivan KD, Steiniger M, Marzluff WF. A core complex of CPSF73, CPSF100, and symplekin may form two different cleavage factors for processing of poly(A) and histone mRNAs. Mol Cell 2009; 34:322-32; PMID:19450530; http://dx.doi.org/10.1016/j.molcel.2009.04.024
39. Benoit B, Juge F, Iral F, Audibert A, Simonelig M. Chimeric human CstF-77/drosophila suppressor of forked proteins rescue suppressor of forked mutant lethality and mRNA 3' end processing in drosophila. Proc Natl Acad Sci U S A 2002; 99:10593-8; PMID:12149458; http://dx.doi.org/10.1073/pnas.162191899
40. Godfrey AC, White AE, Tatomer DC, Marzluff WF, Duronio RJ. The drosophila U7 snRNP proteins Lsm10 and Lsm11 are required for histone pre-mRNA processing and play an essential role in development. RNA 2009; 15:1661-72; PMID:19620235; http://dx.doi.org/10.1261/rna.1518009
41. White AE, Leslie ME, Calvi BR, Marzluff WF, Duronio RJ. Developmental and cell cycle regulation of the drosophila histone locus body. Mol Biol Cell 2007; 18:2491-502; PMID:17442888; http://dx.doi.org/10.1091/mbc.E06-11-1033
42. Su TT, Campbell SD, O'Farrell PH. The cell cycle program in germ cells of the drosophila embryo. Dev Biol 1998; 196:160-70; PMID:9576829; http://dx.doi.org/10.1006/dbio.1998.8855
43. Lanzotti DJ, Kupsco JM, Yang XC, Dominski Z, Marzluff WF, Duronio RJ. Drosophila stem-loop binding protein intracellular localization is mediated by phosphorylation and is required for cell cycle-regulated histone mRNA expression. Mol Biol Cell 2004; 15:1112-23; PMID:14999087; http://dx.doi.org/10.1091/mbc.E03-09-0649
44. Cayirlioglu P, Ward WO, Silver Key SC, Duronio RJ. Transcriptional repressor functions of drosophila E2F1 and E2F2 cooperate to inhibit genomic DNA synthesis in ovarian follicle cells. Mol Cell Biol 2003; 23:2123-34; PMID:12612083
45. Mulligan PK, Rasch EM. Determination of DNA content in the nurse and follicle cells from wild type and mutant drosophila melanogaster by DNA-feulgen cytophotometry. Histochemistry 1985; 82:233-47; PMID:2581922
46. Calvi BR, Lilly MA, Spradling AC. Cell cycle control of chorion gene amplification. Genes Dev 1998; 12:734-44; PMID:9499407
47. Spradling AC, Mahowald AP. Amplification of genes for chorion proteins during oogenesis in drosophila melanogaster. Proc Natl Acad Sci U S A 1980; 77:1096-100; PMID:6767241
48. Schulte J, Tepass U, Auld VJ. Gliotactin, a novel marker of tricellular junctions, is necessary for septate junction development in drosophila. J Cell Biol 2003; 161:991-1000; PMID:12782681; http://dx.doi.org/10.1083/jcb.200303192
49. Fristrom DK. Septate junctions in imaginal disks of drosophila: A model for the redistribution of septa

during cell rearrangement. J Cell Biol 1982; 94:77-87; PMID:7119018

50. Auld VJ, Fetter RD, Broadie K, Goodman CS. Gliotactin, a novel transmembrane protein on peripheral glia, is required to form the blood-nerve barrier in drosophila. Cell 1995; 81:757-67; PMID:7539719; http://dx.doi.org/10.1016/0092-8674(95)90537-5
51. Hofmann I, Schnolzer M, Kaufmann I, Franke WW. Symplekin, a constitutive protein of karyo- and cytoplasmic particles involved in mRNA biogenesis in xenopus laevis oocytes. Mol Biol Cell 2002; 13:1665-76; PMID:12006661; http://dx.doi.org/10.1091/mbc.01-12-0567
52. Mansfield JH, Wilhelm JE, Hazelrigg T. Ypsilon schachtel, a drosophila Y-box protein, acts antagonistically to orb in the oskar mRNA localization and translation pathway. Development 2002; 129:197-209; PMID:11782413
53. Wilhelm JE, Mansfield J, Hom-Booher N, Wang S, Turck CW, Hazelrigg T, Vale RD. Isolation of a ribonucleoprotein complex involved in mRNA localization in drosophila oocytes. J Cell Biol 2000; 148:427-40; PMID:10662770
54. Schotman H, Karhinen L, Rabouille C. dGRASP-mediated noncanonical integrin secretion is required for drosophila epithelial remodeling. Dev Cell 2008; 14:171-82; PMID:18267086; http://dx.doi.org/10.1016/j.devcel.2007.12.006
55. Bilder D, Haigo SL. Expanding the morphogenetic repertoire: Perspectives from the drosophila egg. Dev Cell 2012; 22:12-23; PMID:22264728; http://dx.doi.org/10.1016/j.devcel.2011.12.003
56. Nagaoka K, Udagawa T, Richter JD. CPEB-mediated ZO-1 mRNA localization is required for epithelial tight-junction assembly and cell polarity. Nat Commun 2012; 3:675; PMID:22334078; http://dx.doi.org/10.1038/ncomms1678
57. Lanzotti DJ, Kaygun H, Yang X, Duronio RJ, Marzluff WF. Developmental control of histone mRNA and dSLBP synthesis during drosophila embryogenesis and the role of dSLBP in histone mRNA 3' end processing in vivo. Mol Cell Biol 2002; 22:2267-82; PMID:11884612